



GLOBAL JOURNAL OF HUMAN SOCIAL SCIENCE
GEOGRAPHY & ENVIRONMENTAL GEOSCIENCES
Volume 12 Issue 10 Version 1.0 Year 2012
Type: Double Blind Peer Reviewed International Research Journal
Publisher: Global Journals Inc. (USA)
Online ISSN: 2249-460X & Print ISSN: 0975-587X

Multiyear Analysis of Ground-Based Sunphotometer (AERONET) Aerosol Optical Properties and its Comparison with Satellite Observations over West Africa

By Oluleye A , Ogunjobi K.O , Bernard A , Ajayi V.O & Akinsanola A.A.
Federal University of Technology Akure, Nigeria

Abstract - The Sahelian West Africa (Long 20W:20E, Lat 0:30N) by its climatological and geographical conditions is a key region for the characterization of global atmospheric aerosol optical properties. This study evaluates the spatial and temporal variation of the Aerosol Optical Depth (AOD_{440nm}), aerosol particle size characterization (Angstrom exponent ($\alpha_{440-675nm}$) at four locations (Agoufou, Banizoumbou, Cape Verde and Ilorin) over a period of January 2005 to December 2009. Results of the day-to-day AOD_{440nm} variations as well as the seasonal and annual variations are presented in order to establish the aerosol climatology in the region. We compared satellite derived data of Total Ozone Mapping Spectrometer - Aerosol Index (TOMS-AI), MODIS (Terra and Aqua) with those of ground-based Sunphotometer AERONET measurements. In general, there exists good relationship between MODIS (Terra and Aqua) and the ground-based AERONET measurements with correlation coefficients, $R^2 > 0.8$ reported in all stations. However low coefficients (as low as 0.40) were obtained in all the stations for regressions between TOMS AI and ground-based Sunphotometer AERONET data.

Keywords : AERONET AOD; MODIS; TOMS-AI; Angstrom exponent.

GJHSS-B Classification : FOR Code: 160511 , 160507



Strictly as per the compliance and regulations of:



© 2012. Ogunjobi K.O , Oluleye A , Bernard A , Ajayi V.O & Akinsanola A.A.. This is a research/review paper, distributed under the terms of the Creative Commons Attribution-Noncommercial 3.0 Unported License (<http://creativecommons.org/licenses/by-nc/3.0/>), permitting all non-commercial use, distribution, and reproduction in any medium, provided the original work is properly cited.

Multiyear Analysis of Ground-Based Sunphotometer (AERONET) Aerosol Optical Properties and its Comparison with Satellite Observations over West Africa

Oluleye A^α, Ogunjobi K.O^ο, Bernard A^ρ, Ajayi V.O^ω & Akinsanola A.A.[¥]

Abstract - The Sahelian West Africa (Long 20W:20E, Lat 0:30N) by its climatological and geographical conditions is a key region for the characterization of global atmospheric aerosol optical properties. This study evaluates the spatial and temporal variation of the Aerosol Optical Depth (AOD_{440nm}), aerosol particle size characterization (Angstrom exponent ($\alpha_{440-675nm}$)) at four locations (Agoufou, Banizoumbou, Cape Verde and Ilorin) over a period of January 2005 to December 2009. Results of the day-to-day AOD_{440nm} variations as well as the seasonal and annual variations are presented in order to establish the aerosol climatology in the region. We compared satellite derived data of Total Ozone Mapping Spectrometer - Aerosol Index (TOMS-AI), MODIS (Terra and Aqua) with those of ground-based Sunphotometer AERONET measurements. In general, there exists good relationship between MODIS (Terra and Aqua) and the ground-based AERONET measurements with correlation coefficients, $R^2 > 0.8$ reported in all stations. However low coefficients (as low as 0.40) were obtained in all the stations for regressions between TOMS AI and ground-based Sunphotometer AERONET data.

Keywords : AERONET AOD; MODIS; TOMS-AI; Angstrom exponent.

I. INTRODUCTION

Dust particles appear to be the largest contributor to the column integrated total aerosol optical depth over West Africa. According to D'Almeida (1986), there are four major source areas which contribute to dust aerosols over the region. The first source extends from the Spanish Sahara to the north Mauritania, while the second is located in a triangular zone formed by the Hoggar, Andrar des Iforhas and Air Mountains, i.e. northeast of Geo (Mali). The third source is situated north to northeast of Dirku, north of Bilma (Niger) off the west side of the Tibesti Mountains in Chad Republic while the fourth source is located in the northern part of Sudan. Dust aerosols from these locations have wide range of impacts on visibility and health; modification of rains; reduction of temperature and largely affects the regional climate (Goudie and Middleton 2001). Therefore for comprehensive understand-

ing of the role of aerosols in climate system, their properties, spatial and temporal variations must be properly understood. Hence, it is significant to obtain such information via ground-based monitoring networks such as the Aerosol Robotic Network, AERONET (Holben et al., 1998) and satellite observations such as Total Ozone Mapping Spectrometer (TOMS), Moderate Resolution Imaging Spectro-Radiometer, MODIS (Terra and Aqua), Multiangle Imaging Spectroradiometer (MISR), Polarization and Directionality of the Earth's Reflectance (POLDER) (e.g., El-Metwally et al., 2011; Christopher and Jones 2010; Bennouna et al., 2011; de Meij and Lelieveld, 2011). Ground-based instruments measure local observations while the air borne sensors have the ability to monitor aerosols on a global scale. Satellite-based remote sensing plays a vital role in gaining good knowledge and understanding of global aerosol variations and their interaction within the earth's climate (Kaufman et al., 2002). Satellite data have long been employed for aerosol studies however with some major challenges in almost every step of the retrieval process, such as, sensor calibration, cloud screening, corrections for surface reflectivity and variability of aerosol properties; size distribution, refractive index (King et al., 1999; Bennouna et al., 2011). Consequently, significant differences exist among various aerosol products generated from different sources e.g., AVHRR (Ignatov and Stowe, 2002; Ignatov et al., 2004), the MODIS (Remer et al., 2005), the Total Ozone Mapping Spectrometer (TOMS) (Torres et al., 1998; 2002), the Polarization and Directionality of the Earth's Reflectance (POLDER) instrument (Goloub et al., 1999; Deuzé et al., 2001), and the Multiangle Imaging Spectroradiometer (MISR), (Kahn et al., 2001) etc. A compilation of more than 2 decades of TOMS-AI data provided a more precise identification of tropospheric aerosol characteristics surrounding distinct source areas and long-range transport over continents and oceans (e.g., Chiapello and Moulin, 2002; Moulin and Chiapello, 2004). Myhre et al. (2004) compared a large number of global aerosol products and revealed the general features of agreement and discrepancies. However, insights into the causes of the discrepancies

Author α: Oluleye A. Department of Meteorology Federal University of Technology Akure, Nigeria. E-mail : oluleyea@gmail.com

were lacking and the state-of-the-art aerosol product from the MODIS was excluded from their work. Comparing simulated and observed Aerosol Indices (AIs) in the near-ultraviolet, in West Africa Yoshioka et al. (2005) found that the best comparison at the Sahara-Sahel border is obtained by adding 20%-25% of dust from disturbed soils. The seasonal character of the aerosol flux especially its link with the harmattan dust at some locations in West Africa and the implications on weather and climate have been a subject of increasing interest to researchers (e.g. Holben et al., 2001; Dobovik et al., 2002; Adeyewa and Balogun, 2003; Ogunjobi et al., 2007; Ogunjobi et al., 2008). The objective of this study therefore is to document the long term seasonal and inter-annual variability of aerosol loading over Sahelian West Africa. It presents a comparison between Total Ozone Mapping Spectrometer Aerosol Index, MODIS AOD (Terra and Aqua) and the ground-based Sunphotometer AERONET AOD observations in four different locations in the region. The study further investigates the agreement and differences between the data sets while regression equations of the satellite derived data and the ground-truth were also presented in order to determine whether satellite measurements can adequately reproduce aerosol optical depth for the region.

II. STUDY AREA AND METHODS

a) Climate of the study region

The regional map showing the locations of the AERONET Sunphotometers, TOMS Aerosol Index, and MODIS AOD data utilized in this study is shown in Figure 1. Results from daily observations from period January 2005- December 2009 at three West Africa sites and a location in the Atlantic Ocean is herewith presented. The stations under-study include Agoufou; Mali (15°21'N, 1°29'W), Banizoumbou; Niger (13° 45'N, 02° 39'E), and Cape Verde; Tropical Atlantic Ocean (16° 45'N, 22° 57'W); Ilorin; Nigeria (08° 32'N, 04° 34'E). The four stations differ in terms of their annual precipitation, temperature and relative humidity (see Table 1). The annual total precipitation values averaged over each month during this period were 333.0 mm/yr, 540.8 mm/yr, 69.5 mm/yr and 1185.0 mm/yr in Agoufou, Banizoumbou, Cape Verde and Ilorin respectively. Dry season starts in Agoufou from October and ends in May of the following year while the rainy season is June through September. Beginning in October, the harmattan trade wind blows sand, grit and dry air over the station with the hottest time of the year between March-June (Table 1). Banizoumbou is located in the Sahel region, between the Sahara desert to the north and the Sudanian zone to the south. The aerosol climate in Banizoumbou is influenced by the dry harmattan winds, an easterly or north easterly wind laden with dust transported from the Sahara during the dry months of

November to March of the following year. The relative humidity during the *harmattan* months in Banizoumbou varies between 20-31% (Table 1). Cape Verde is located in the mid-Atlantic Ocean some 570 km off the west coast of Africa. The landscape varies from dry plains to high active volcanoes with cliffs rising steeply from the ocean. The climate is arid as December-June is cool and dry, with temperatures at sea level averaging 24 °C; July-November is warm and dry, with temperatures averaging 26°C. During the dry season (DJF), windstorms blowing from the Sahara sometimes form a dense dust cloud that characterizes the station. Although some rain comes during the latter season, rainfall is however sparse all over the year and very erratic. Ilorin is situated in the Guinea Savannah zone of West Africa; a transition zone between the Guinea coast and Sahelian West Africa. Ilorin is in the desert transition zone between the Sahara and the savanna of upper Nigeria and is influenced by the dusty harmattan wind (Ginoux et al., 2010). It is characterized by persistent conditions of high aerosol loading as well as intense dust outbreaks that affect the local climate during the *harmattan* season of November to March of the following year. The climate is a transition between the equatorial rain forest in the south and the Sahel Savannah in the north. The hot dry season commences from about the middle of October to late March when the North-Easterly (NE) winds from the Sahel dominates the climate pattern. The rainfall amount during the harmattan season ranges between 4.6mm/yr in November to 57.4mm/yr in March as shown in Table 1). However during the wet season from April to mid October, the climate is dominated by the South-Westerly winds from the Atlantic Ocean characterized with high relative humidity between 75% to 80%.

b) Instrumentation

AERONET an acronym of AERosol NETwork is a federated network of CIMEL Sunphotometers. Since 1994, fourteen (14) stations have been installed in West Africa by the PHOTONS component of the AERONET network, with different periods and durations of observations. This network of instruments have allowed the establishment of the seasonal cycle of the vertically integrated content (Aerosol Optical Depth, AOD) of mineral dust and biomass burning in different stations of West Africa (Holben et al., 2001). AERONET data are widely used as a reference for satellite validation and model evaluation studies, because the measurement characteristics are well understood and documented (Dobovik et al., 2000). The direct sun measurements are made every 15 minutes in eight spectral channels at 340, 380, 440, 500, 675, 870, 940 and 1020 nm (nominal wavelengths). The CIMEL Sunphotometer is a solar-powered, hardy, robotically pointed sun and sky spectral radiometer. The diffuse sky radiances, called almucantar, is a series of measurements taken at the

elevation angle of the Sun for specified azimuth angles relative to the position of the Sun. During almucantar measurements, observations from a single channel are made in a sweep at a constant elevation angle across the solar disc and continue through 360° of azimuth in about 40s. This is repeated for each channel to complete an almucantar sequence. A detailed description of the AERONET instrumentation can be found in Holben *et al.* (1998).

The AERONET site at Agoufou is located in a sand dunes area (grazing land) 30 km from Hombori while that of Banizoumbou location is located on a small isolated plateau in a cultivated sandy area near the village of Banizoumbou, 60 km east from Niamey. In addition, the location of the AERONET instrument in Banizoumbou was temporarily changed (~100m) during June-July 2006; and June 2007 and thus no data are available for these few days when displacement occurred (Marticorena *et al.*, 2010). The calibrations of the Sun photometers in the AERONET sites were performed regularly at the Goddard Space Flight Center (GSFC) resulting in high accuracy AOD of ~0.01 in the visible and near-infrared and ~0.02 in the ultraviolet (Eck *et al.*, 1999), Data are quality checked and cloud-screened following the methodology of Smirnov *et al.* (2000). TOMS - Aerosol Index (AI) constitutes one of the most useful space-borne data sets, offering long-term daily global information on UV absorbing aerosol (black carbon, desert dust) distributions (Torres *et al.*, 1998). The TOMS on Nimbus-7 provided global measurements from November 1978 to December 1994. The earth Probe (EP) TOMS was launched on 2 July 1996 to provide supplementary measurements while the Aura-OMI algorithms is been available since 2004 to present. TOMS Aerosol Index is not a physical parameter but an index of aerosol that is sensitive to aerosol height (Torres *et al.*, 1998). It is defined as a measure of the change of spectral contrast in the near ultra violet (341 and 380nm) due to radiative transfer effect of aerosols in a Rayleigh scattering atmosphere. By definition, AI is positive for absorbing aerosols, near zero (± 0.2) in the presence of clouds or large size (0.2 μ m or larger) nonabsorbing aerosols and negative for small size non absorbing aerosols. TOMS AI is therefore regarded as one of the potential sources for monitoring dust transport characteristics

The MODERate resolution Imaging Spectro radiometer (MODIS) has one camera, measuring irradiances in 36 spectral bands from 0.4 μ m-14.5 μ m with spectral resolution of 250m (bands 1-2), 500m (bands 3-7) and 1000m (bands 8-36) (de Meij and Lelieveld, 2011). The first MODIS instrument was lunched at the end of 1999 on board the polar orbiting Terra spacecraft, and has been acquiring daily global data since February 2000. The MODIS AOD_{440nm} over the stations under study are the standard Terra -MODIS level 2 and Aqua MODIS level 2 aerosol product

MOD04(collection 005). It should be noted that in addition to the Terra MODIS AOD_{440nm} products, we also used the MODIS Aqua AOD_{440nm} products as well which are processed with the Deep Blue algorithm (Hsu *et al.*, 2004). The Deep Blue retrieval provides AODs over bright surfaces including the desert regions. The difference between the MODIS Terra and Aqua algorithm and Deep Blue is that the former aerosol retrieval is based on a dark surface approach.

III. RESULTS AND DISCUSSION

a) Aerosol optical depth (AOD_{440nm}) and Angstrom exponent ($\alpha_{440-675nm}$) Climatology

In this section, the day-to-day as well as the monthly variation of AERONET AOD_{440nm} and $\alpha_{440-675nm}$ are presented in order to establish the different aerosol climatologies over the region. Figures 2a-d show the cloud free daily mean AOD_{440nm} values at Agoufou (2005-2008), Banizoumbou (2005-2009), Cape Verde (2005-2009) and Ilorin (2005-2009). The plot of daily mean AOD_{440nm} for Agoufou represented by 1092 cloud free days indicate relative small day-to-day variations in the measurement period shows in figure 2a. However, in the months of February to May, AOD_{440nm} values shows large variations when it showed its obtainable maximum values while minimum AODs are obtainable between the months of October to December as well as July to August. The highest AOD was recorded in the year 2005 with an average daily value of 0.60 ± 0.34 followed by that of 2007 (0.56 ± 0.48) while the least was recorded in 2008 (0.47 ± 0.33). Figure 2b provides similar time series plot in order to assess the temporal distribution of aerosols in Banizoumbou. Unlike Agoufou, Banizoumbou shows large day-to-day variability in AOD which may be attributed to large variations of aerosol particle in combination with large variability in meteorological conditions such as windspeed and direction, atmospheric stability and accumulation of aerosols in the boundary layer (Masmoudi *et al.*, 2003; Kambezidis and Kaskaoutis, 2008). The largest day-to-day variation was noted mostly during the dry months of every year while the rainy season shows small variation due to scavenging action of precipitation (Ogunjobi *et al.*, 2008). Small variability is observed in the day-to-day variation of AOD almost throughout the year in Cape Verde (Figure 2c). The AODs are generally low while occasional high values correspond to desert-dust aerosol in agreement with similar study of Kambezidis and Kaskaoutis (2008) for a remote Island of Nauru in the Pacific Ocean. Few days of high AOD were noted during the dry harmattan months of December to March the following year each year while major peaks were recorded in the summer months of June- August. During most of the year in Cape Verde the North Atlantic between 20-30°N is dominated by high pressure. South of 25°N wind is generally from the east transporting dust and biomass

burning aerosols westward into the Atlantic (Christopher and Jones, 2010). The produced maritime sea-spray aerosol components under strong sea surface winds lead to additional source of variations in the AOD reported in Cape Verde (Setheesh et al., 2006). At Ilorin the AOD is dominated by pronounced seasonal variations and marked increase in AOD values from December to March with peak daily values observed in the months of January-March of following year (Figure 2d). From November – December/January -March, large aerosol amounts (average optical depth >1.0 near the source regions) are generated by intense Saharan dust outbreaks and occasionally biomass-burning activities in the region. Ginoux et al. (2010) reported that during the dry season in the arid region of West Africa south of 20°N, from December to February, dust sources are very active while at the same time large amount of carbonaceous aerosols are emitted by biomass burning.

Figures 3a-d show the day-to-day spatial variations of the Angstrom exponent, $\alpha_{440-675\text{nm}}$ for 440-675nm indicating large day-to-day variations in all stations. It is interesting to note that the variations are larger at low AODs when fine –mode aerosols dominate over the optical influence of the large coarse mode particles. For example in Agoufou (Figure 3a) high variations of $\alpha_{440-675\text{nm}}$ are noted under low AOD between February–June. Also observed are high $\alpha_{440-675\text{nm}}$ during the dry season when AOD are equally high indicative of the presence of biomass burning aerosols in the location (Eck et al., 2001b). The long term daily averages of $\alpha_{440-675\text{nm}}$ were 0.25 ± 0.20 , 0.33 ± 0.25 , 0.67 ± 0.37 and 0.30 ± 0.22 for Agoufou, Banizoumbou, Ilorin and Cape Verde respectively. The values were lower than that reported by Eck et al.(1998) for smoke aerosol in Brazil. The variability of $\alpha_{440-675\text{nm}}$ noted in the stations may be attributed to variability in the size of the smoke particle proportional to the phase of the fire (Eck et al., 2001b), coagulation, humidification process and mixing of fresh smoke particles with other aerosols such as dust and urban pollution (Kaufman , 1998).

Figure 4 shows the frequency distribution of AOD_{440nm} and $\alpha_{440-675\text{nm}}$ for Cape Verde, Ilorin, Banizoumbou and Agoufou which is used to characterized aerosol load at the different sites. Also shown as insert is the line plots of AOD_{440nm} and $\alpha_{440-675\text{nm}}$ with their $\pm 5\%$ standard deviation. Figure 4a shows that 98%, and 76%, of the AOD falls within the range 0.5-1.0 in Cape Verde and Ilorin respectively, while 82% and 89% in Banizoumbou and Agoufou respectively. It is further noted in figure 4a that only 0.5%, 0.4% and 0.3% of the AOD falls within the range of values 3.5- 4.0 in Ilorin, Banizoumbou and Agoufou respectively while Cape Verde does not have any value within this magnitude. The result here is in agreement with the earlier work of Ogunjobi et al.(2008) for the same region during an observation periods of 1999-2005. In all

stations under consideration, $\alpha_{440-675\text{nm}}$ frequency distribution shows that inverse relationship exist between the AOD and Angstrom exponent with the exception of Ilorin. For example, 89%, 51%, 86%, and 92 % of the Angstrom exponent falls within 0.2-0.6 in Cape Verde, Ilorin, Banizoumbou and Agoufou respectively. The result shows that 8.0% and 0.3% falls within the range greater than 1.4 in Ilorin and Banizoumbou while Cape Verde and Agoufou does not have records of any Angstrom exponent within the range. An interesting feature of Figure 4b shows that at Ilorin only 5% of the Angstrom exponent falls in the range ≤ 0.2 while other stations has values greater than 40%. The Angstrom exponent dependence on aerosol optical depth has been used by several authors (e.g. Cachorro et al., 2001; Ogunjobi et al., 2008; Cheng et al., 2006; Kaskaoutis et al., 2007) to determine different aerosol types for specific location through determining of physical interpretable cluster regions.

Figure 5 shows the relationship between AOD and Angstrom exponent the in order to determine the dependence of aerosol loading on particle size. In general it is observed that $\alpha_{440-675\text{nm}}$ is low when AOD_{440nm} is comparatively high. In Agoufou, there is a wide range of $\alpha_{440-675\text{nm}}$ values at low AOD_{440nm} (<0.5) with $\alpha_{440-675\text{nm}}$ varying between near zero to 1.19 (Figure 5a). This suggests that under relatively clean atmospheric conditions very different aerosol types can be found over Agoufou (from pure fine-mode pollutants to coarse-mode particles). There is a slight reduction of $\alpha_{440-675\text{nm}}$ as AOD_{440nm} increases which reflect the transition of fine-mode particles to accumulation-mode through coagulation, condensation and gas-to-particle conversion. At Banizoumbou (Figure 5b) an increase in the values of $\alpha_{440-675\text{nm}}$ with corresponding increase in AOD_{440nm} indicated the contribution of fine fresh smoke particles in the atmosphere during episodes of biomass burning or mixture of smoke and other aerosols such as desert dust and urban pollution. The scatter-plot for Cape Verde shows high dispersion at low AOD suggesting that under relatively clean maritime atmospheric condition different aerosol types can be found in Cape Verde ranging from sea salt pollutants to desert dust aerosols (Figure 5c). The increasing values of α with increasing AOD_{440nm} indicate the significant contribution of fine “fresh-smoke” particles in the atmospheric column, especially under high turbidity at Ilorin (Figure 5d). During the period of measurements $\alpha_{440-675\text{nm}}$ computed in Agoufou and Cape Verde were observed to change less over a wide range of aerosol optical depth than in Banizoumbou and Ilorin which indicated more of coarse-mode particles in the two latter stations. There is a noted reduction of $\alpha_{440-675\text{nm}}$ as AOD_{440nm} increases in Cape Verde; thus reflecting the transition from the fine-mode particles to accumulation mode of mixed type aerosols through coagulation,

condensations and gas-to-particle conversion. Majority of the points in all the stations confines in the area corresponding to higher $\alpha_{440-675\text{nm}}$ values for $\text{AOD}_{440\text{nm}} \leq 1.0$, confirming the presence of fine mode particle of biomass burning, urban pollution, mixed type pollutants origin. However, there are also large population of points corresponding to low $\alpha_{440-675\text{nm}}$ and high AOD indicating presence of mineral dust aerosols especially in Banizoumbou and Ilorin. In general, despite the large scatter of data points in all stations (Figures 5a-d), $\alpha_{440-675\text{nm}}$ values decrease with increasing AOD. This further indicates that coarse aerosols dominate and also that the ratio of coarse/fine aerosols increases, under conditions of high turbidity. The generalized trend noted in this region in good agreement with the observed pattern at several other locations for different aerosol types (e.g., Eck et al., 2001a; 2001b; Masmoudi et al., 2003; Cheng et al., 2006; Kaskaoutis et al., 2007).

b) Satellite (MODIS, TOMS-AI) and AERONET ground-based measurements intercomparison

Analyses of the AERONET $\text{AOD}_{440\text{nm}}$ profile, TOMS $\text{AI}_{340\text{nm}}$, and MODIS 440nm for the four locations are shown in Fig. 6a-d. For consistency we choose the 440nm AERONET and MODIS channel because the 340 and 380nm wavelength channels are not available at all sites. For large particles like dust Bounhir et al. (2008) stated that the wavelength dependence between 340 nm and 440nm is very small and as such the 440nm AOD values is approximately equal to that of 340nm. Ground-based AERONET, TOMS-AI and MODIS AOD show extreme similarity in their daily variations. For example, Agoufou has $\text{AOD}_{440\text{nm}}$ values of 3.88, 3.80 and 2.62 on 26th May 2006, 3rd and 4th May 2007 respectively which corresponds to TOMS AI and MODIS- Terra however no MODIS-Aqua retrievals were available (Figure 6a). Analysis of AERONET AODs at Banizoumbou during 2005-2007 also shows strong agreement with TOMS AI, and MODIS data (Figure 6b). For example on 5th April, 2007 AERONET AOD, MODIS (Terra and Aqua) and TOMS AI, were 2.51, 2.50, 2.50 and 2.80 respectively which yielded a difference of only 0.40% for MODIS terra and Aqua; 11.60% for TOMS AI when compared with ground-based AERONET AOD measurement. Figure 6d shows that both satellite and ground based instruments captured the high aerosol loading at Ilorin in March 2006, January 2007 and February 2008. The average aerosol optical depths at Ilorin during the dry harmattan months of December 2005 to March of 2006 were 1.11, 1.14, 1.17 and 1.02 for AERONET AOD, TOMS AI, MODIS Terra and Aqua respectively. The corresponding statistics of daily AERONET, TOMS AI, MODIS-Terra and Aqua are shown in Tables 2 - 5 respectively. Also shown are the number of cloud free days in each station as well as the 5th and 95th percentile lower (LCL) and upper (UCL) confidence levels. For example the P5 LCL and UCL at Ilorin was

0.243 and 0.244 respectively while the average AOD is 0.75 ± 0.49 . Table 2 shows the mean AERONET $\text{AOD}_{440\text{nm}}$ in Agoufou is 0.52 ± 0.39 as compared to 0.57 ± 0.43 , 0.37 ± 0.24 and 0.75 ± 0.49 at Banizoumbou, Cape Verde and Ilorin respectively. The annual mean of AOD estimated for Cape Verde is much higher than the annual value of 0.07 reported by Kambezidis and Kaskaoutis (2008) for a Pacific Island station of Nauru between 2002-2004. The variance (u) of the mean values of TOMS AI at Agoufou, Banizoumbou, Cape Verde and Ilorin as shown in Table 3 yielded 0.11, 0.17, 0.21 and 0.29 respectively which is observed to be very close to the 5th percentile lower and upper confidence levels. Tables 4 and 5 show the averages of MODIS-Terra and Aqua at Agoufou were 0.56 and 0.57 respectively.

The monthly variations for AERONET $\text{AOD}_{440\text{nm}}$, TOMS AI, MODIS-Terra and Aqua AOD are presented in Figures 7a-d as well as the 5 % standard deviation for each month. In Agoufou, AOD increased from February with peak values in May/ June, from the later onset of rainfall in June, after which once again, the increasing rainfall decreases aerosol load (Figure 7a). Banizoumbou recorded high AODs in March (AERONET, MODIS) with a secondary peak in June (Figure 7b) while AOD showed slight monthly variation at Cape Verde with highest AOD was observed in June-July (Figure 7c). The observed seasonal peak in March in Banizoumbou may be attributed to the long-range transport of primarily Saharan aerosols believed to be mainly from sources located in Niger, south Algeria, Libya and Chad (Holben et al., 2001). Results presented in Figure 7d indicate that $\text{AOD}_{440\text{nm}}$ from ground-based AERONET and Satellite sensors at Ilorin are maximal in the dry cold months of December-March and drastically reduces to minimal at the onset of rains in April through September caused jointly by increase washout owing to the gradient of increasing precipitation and the location of source regions for the dust.

The previous discussion showed that the observations of AERONET $\text{AOD}_{440\text{nm}}$, TOMS-AI and AOD retrieved from MODIS-Terra/Aqua were relatively in good qualitative agreement. For the same data set Figure. 8a-d shows the regression plots of TOMS AI, MODIS-Terra and Aqua against ground based AERONET AOD. Linear regression expressions in the form of $\text{AOD}_{\text{satellite}} = m * \text{AOD}_{\text{AERONET}} + c$ where obtained for the region. Summary of the AERONET AOD with TOMS AI, MODIS-Terra and Aqua linear relationships from daily observations are presented in Table 6. Also computed are the corresponding number of days, correlation coefficients, and standard errors in the slopes and intercepts.

Figure 8 shows that TOMS AI and MODIS-derived AODs are well correlated with ground-based observations in all stations although TOMS AI retrieval shows weak correlations at Banizoumbou and Cape

Verde (Table 6). The correlation between MODIS- Terra and Aqua and AERONET AOD_{440nm} is >0.80 in all stations while the correlation with TOMS- AI yielded 0.52 and 0.58 in Agoufou and Ilorin respectively and weaker correlation of 0.45 and 0.40 at Banizoumbou and Cape Verde respectively (Table 6). Low correlation coefficient observed in Banizoumbou can be explained by a combination of various factors such as sensitivity of the TOMS algorithm to altitude of the mineral dust layer, sub-pixel cloud contamination, aerosol composition, size distribution and sampling frequency for the Sunphotometer and TOMS algorithm (Toress et al., 2002; Kubilay et al., 2005). Figure 8 further shows that TOMS- AI is biased at low AOD values, which may be associated with a sensor calibration error or an improper assumption about ground surface reflection (Zhao et al., 2002); in addition, large errors in surface reflectance could also lead to large intercepts (Chu et al., 2002). A slope that is different from unity indicates that there may be some inconsistency between aerosol microphysical and optical properties used in the retrieval algorithm and that in the real situation (Zhao et al., 2002). For example slope lower than unity recorded in all the stations indicates an underestimation of AERONET AOD with respect to TOMS- AI retrieval. This is in agreement with the work of Myhre et al. (2005) that reported a tendency for the aerosol satellite retrievals to have higher AODs than the AOD from the Sunphotometers for low AOD and vice versa for high AODs. Hsu et al. (1999) shows that TOMS-AI measurements are linearly proportional to the AOD derived from independent ground based Sunphotometers instruments over regions of biomass burning and Africa dust. Their findings demonstrated that AI depends on aerosol optical thickness, single scattering albedo, aerosol layer height and viewing geometry. Ginoux and Torres, (2003) develops an empirical relationship to express TOMS AI for dust plumes as an explicit function of four quantities; single scattering albedo, AOD, surface pressure and altitude of dust plume. However, the strong dependence of AI on height distribution of aerosol decreases its sensitivity to the aerosol presences at altitude below 1.5km (Bounhir et al., 2008). Torres et al. (2002) confirms the good agreement between TOMS- AI and AERONET data for mineral, carbonaceous and sulphate aerosols. Bounhir et al. (2008) reported Pearson correlation coefficient varying from 0.68 to 0.92 between AERONET data and satellite derive aerosol optical depth (MODIS, MISR and TOMS OMI) for Morocco. The high coefficients of determination between the AERONET AOD_{440nm} values and satellite derive aerosol loading (TOMS- AI and MODIS) indicate a rather successful method of estimation of the AOD from TOMS- AI, and MODIS observation in Sahelian West Africa. This is really instructive especially for a region where ground observations are difficult to come-by.

IV. CONCLUSION

The study presents an analysis of the spatial, seasonal and interannual variability in absorbing aerosol loading over sahelian West Africa detected by satellite (MODIS and TOMS) and ground-based AERONET Sunphotometer sensors during 2005-2009. In general the daily, monthly and annual means of MODIS (Terra & Aqua) and TOMS retrieved AOD/AI are in good agreement with ground-based AERONET data. An important conclusion of this result is the creation of large data base from satellite and AERONET federation Network for the Sahelian West Africa. The seasonal cycle in aerosol optical depth corresponded to the seasonal variability in dust, biomass burning and mixed aerosol emission during the harmattan dry period to the dust free rainfall season. The aerosol optical depth showed large variation with high values during the harmattan dry months and low values during the rain/monsoon season. The mean and standard values of the Angstrom exponent were found to be lower during high dust hazy season (high AOD) except for occasional biomass burning episodes when high AOD corresponds to high Angstrom exponent. The AERONET data have been identified useful for validation purposes for the satellite data over the region. The results are confirmed by the plots of the regression comparison between ground-based AERONET and corresponding satellite daily data. The time series of the AOD retrieved from MODIS and TOMS are in good agreement with ground-based AERONET measurements, with correlation coefficients of >0.80 estimated in all stations for correlation between MODIS and AERONET retrieved AODs. Such study are important for improving aerosol parameterizations in radiative transfer models and evaluating the regional aerosol radiative forcing.

V. ACKNOWLEDGEMENTS

The authors wish to express their sincere thanks to the NASA/GSFC TOMS Ozone processing team and the principal investigator of the AERONET sites used in this study. We wish to also acknowledge the International Center for Theoretical Physics (ICTP), Trieste, Italy that provides accessibility to literatures used for this research output via the electronic journal delivery service (ejds).

REFERENCES RÉFÉRENCES REFERENCIAS

1. Adeyewa, Z.D., Balogun, E.E., 2003. Wavelength dependence of aerosol optical depth and the fit of the Angstrom law. *Theor. Appl. Climatol.* 74, 105–122.
2. Andreae, M.O., Schmid, O., Yang, H., Chand, D., Yu, J.Z., Zeng, L.M., & Zhang, Y.H. (2008). Optical properties and chemical composition of the

- atmospheric aerosol in urban Guangzhou, China. *Atmospheric Environment*, 42, 6335–6350.
3. Bennouna, Y.S., Cachorro, V.E., Toledano, C., Berjón, A., Prats, N., Fuertes, D., Gonzalez, R.,
 4. Rodrigo, R., Torres, B., & de Frutos, A.M. (2011). Comparison of atmospheric aerosol climatologies over southwestern Spain derived from AERONET and MODIS. *Remote Sensing of Environment*, 115, 1272–1284.
 5. Bounhir, A., Benkhaldoun, Z., Mougenot, B., Sarazin, M., Siher, E., & Masmouli, L. (2008). Aerosol column characterization in Morocco: ELT prospect. *New Astronomy*, 13, 41–52.
 6. Cachorro, V. E., Vergaz, R., & de Frutos, A. M. (2001). A quantitative comparison of Angstrom turbidity parameter retrieved in different spectral ranges based on spectroradiometer solar radiation measurements. *Atmospheric Environment*, 35, 5117–5124.
 7. Cheng, T., Wang, H., Xu, Y., Li, H., & Tian, L. (2006). Climatology of aerosol optical properties in Northern China. *Atmospheric Environment*, 40, 1495–1509.
 8. Chu, D.A., Kaufman, Y.J., Ichoku, C., Remer, L.A., Tanré, D., & Holben, B.N. (2002). Validation of MODIS aerosol optical depth retrieval over land. *Geophysical Research Letters*, 29 (12), 29.8007, doi: 10.1029/2001GL013205, 1–2.
 9. Chiapello, I., & Moulin, C. (2002). TOMS and METEOSAT satellite records of the variability of Saharan dust transport over the Atlantic during the last two decades (1979–1997), *Geophysical Research Letters*, 29(8), 1176, doi: 10.1029/2001GL013767.
 10. Christopher, S. A., & Thomas, A. J. (2010). Satellite and surface-based remote sensing of Saharan dust aerosols. *Remote Sensing of Environment*, 114, 1002–1007.
 11. D'Almeida G.A. (1986). A model for Saharan dust Transport. *Journal of Climate and Applied Meteorology*, 25, 903–916.
 12. de Meij, A., & Lelieveld, J. (2011). Evaluating aerosol optical properties observed by ground-based and satellite remote sensing over the Mediterranean and the Middle East in 2006. *Atmospheric Research*, 99, 415–433.
 13. Deuzé, J. L., Bréon, F. M. , Devaux, C. , Goloub, P. , Herman, M. , Lafrance, B., Maignan, F. , Marchand, A., Nadal, F. , Perry, G., & Tanré, D. (2001). Remote sensing of aerosols over land surfaces from POLDER-ADEOS-1 polarized measurements. *Journal of Geophysical Research*, 106, 4913–4926.
 14. Dubovik, O., Smirnov, A., Holben, B.N., King, M.D., Kaufman, Y.J., Eck, T.F., & Slutsker, I., (2000). Accuracy assessments of aerosol optical properties retrieved from Aerosol Robotic Network (AERONET) sun and sky radiance measurements. *Journal of Geophysical Research*, 105, 9791–9806.
 15. Dubovik, O., Holben, B., Eck, T.F., Smirnov, A., Kaufman, Y.J., King, M.D., Tanré, D., & Slutsker, I. (2002). Variability of absorption and optical properties of key aerosol types observed in worldwide locations. *Journal of the Atmospheric Sciences*, 59, 590–608.
 16. Eck, T. F., Holben, B. N., Slutsker, I., & Setzer, A. (1998). Measurements of irradiance attenuation and estimation of aerosol single scattering albedo for biomass burning aerosols in Amazonia. *Journal of Geophysical Research*, 103, 31865–31878.
 17. Eck, T.F., Holben, B.N., Dubovik, O., Smirnov, A., Slutsker, I., Lobert, J.M., & Ramanathan, V. (2001a). Column-integrated aerosol optical properties over the Maldives during the northeast monsoon for 1998–2000. *Journal of Geophysical Research*, 106, 28555–28566.
 18. Eck, T.F., Holben, B.N., Ward, D.E., Dubovik, O., Reid, J.S., Smirnov, A., Mukelabai, M.M., Hsu, N.C., O' Neill, N.T., & Slutsker, I. (2001b). Characterization of the optical properties of biomass burning aerosols in Zambia during the 1997 ZIBBEE field campaign. *Journal of Geophysical Research*, 106 (D4), 3425–3448.
 19. El-Metwally, M., Alfaro, S.C., Abdel Wahab, M.M., Zakey, A.S., & Chatenet, B. (2011). Seasonal and inter-annual variability of the aerosol content in Cairo (Egypt) as deduced from the comparison of MODIS aerosol retrievals with direct AERONET measurements. *Atmospheric Research*, 97, 14–25.
 20. Ginoux, P., & Torres, O. (2003). Empirical TOMS index for dust aerosol: Applications to model
 21. validation and source characterization. *Journal of Geophysical Research*, 108(D17), 4534, doi: 10.1029/2003JD003470.
 22. Ginoux, P., Garbuzov, D., & Hsu, N.C. (2010). Identification of anthropogenic and natural dust sources using Moderate resolution Imaging Spectrometer (MODIS) deep blue level 2 data. *Journal of Geophysical Research*, 115, D05204 (1–10), doi: 10.1029/2009JD012398.
 23. Goudie, A. S., & Middleton, M. J. (2001). Saharan dust storms, nature and consequences.
 24. *Earth-Science Reviews*, 56, 179–204.
 25. Goloub, P., Tanré, D., Deuzé, J.L., Herman, M., Marchand, A., & Bréon, F.M. (1999). Validation of the first algorithm applied for deriving the aerosol properties over ocean using the POLDER/ADEOS measurements. *IEEE Transactions on Geosciences and Remote Sensing*, 37(3), 1586–1596.
 26. Hignett, P., Taylor, J., Francis, P., & Glew, M. (1999). Comparison of observed and modeled direct aerosol forcing during TARFOX. *Journal of Geophysical Research*, 104, 2279–2287.
 27. Holben, B. N., Eck T.F., Slutsker I., et al. (1998). AERONET—A federated instrument network and

- data archive for aerosol characterization. *Remote Sensing of Environment*, 66, 1–16.
28. Holben, B. N., Tanre, D., Smirnov, A., Eck, T. F., Slutsker, I., Abuhassan, N., Newcomb, W. W., Schafer, J., Chatenet, B., Lavenu, F., Kaufman, Y. J., Vande Castle, J., Setzer, A., Markham, B., Clark, D., Frouin, R., Halthore, R., Karnieli, A., O'Neill, N. T., Pietras, C., Pinker, R. T., Voss, K., & Zibordi, G. (2001). An emerging ground-based aerosol climatology: Aerosol Optical Depth from AERONET. *Journal of Geophysical Research*, 106(D11), 12067–12098.
 29. Hsu, N.C., Tsay, S.-C., King, M.D., & Herman, J.R., (2004). Aerosol properties over bright-reflecting source regions. *IEEE Transactions on Geoscience and Remote Sensing*, 42 (3), 557-568.
 30. Hsu, N.C., Herman, J.R., Torres, O., Holben, B.N., Tanre, D., Eck, T.F., Smirnov, A., Chatenet, B., & Lavenu, F. (1999). Comparison of the TOMS aerosol index with sun photometer aerosol optical thickness: Results and Applications. *Journal of Geophysical Research*, 104 (D6), 6269–6279.
 31. Ignatov, A., & Stowe, L. (2002). Aerosol Retrievals from Individual AVHRR Channels: I. Retrieval Algorithm and Transition from Dave to 6S Radiative Transfer Model. *Journal of Atmospheric Science*, 59, 3(1), 313-334.
 32. Ignatov, A., Sapper, J., Laszlo, I., Nalli, N., & Kidwell, K. (2004). Operational Aerosol Observations (AEROBS) from AVHRR/3 onboard NOAA-KLM satellites. *Journal of Atmospheric and Oceanic Technology*, 21, 3.26.
 33. Jacobson, M. (2000). A physically based treatment of elemental carbon optics: Implications for global direct forcing of aerosols. *Geophysical Research Letter*, 27, 217– 220.
 34. Kahn, R., Banerjee, P., & McDonald, D. (2001) The Sensitivity of Multiangle Imaging to Natural Mixtures of Aerosols Over Ocean, *Journal of Geophysical Research*, 106, 18219-18238.
 35. Kaskaoutis, D.G., Kambezidis, H.D., Hatzianastassiou, N., Kosmopoulos, P.G., & Badarinath, K.V.S. (2007). Aerosol climatology: on the discrimination of aerosol types over four AERONET sites. *Atmospheric Chemistry and Physics Discussion*, 7, 6357–6411.
 36. Kaufman, Y. J., Tanre, D., & Boucher, O. (2002). A satellite view of aerosols in the climate system. *Nature*, 419, 215– 223.
 37. Kambezidis, H.D., & Kaskaoutis, D.G. (2008). Aerosol climatology over four AERONET sites: An overview. *Atmospheric Environment*, 42, 1892–1906.
 38. Kim, S.W., Yoon, S.C., Kim, J., & Kim, S.Y. (2007). Seasonal and monthly variations of columnar aerosol optical properties over east Asia determined from multi-year MODIS, LIDAR, and AERONET Sun/sky radiometer measurements. *Atmospheric Environment*, 41, 1634–1651.
 39. Kim, S.W., Choi, I.J., & Yoon, S.C. (2010). A multi year analysis of clear sky aerosol optical properties and direct radiative forcing at Gosan, Korea (2001-2008). *Atmospheric Environment*, 95, 279-287.
 40. King, M.D., Byrne, D.M., Herman, B.M., & Reagan, J.A. (1978). Aerosol size distributions obtained by inversion of spectral optical depth measurements. *Journal of Atmospheric Science*, 35, 2153–2167.
 41. King, M.D., Kaufman, Y.J., Tanre, D., & Nakajima, T. (1999). Remote sensing of tropospheric aerosols from space: Past, present, and future. *Bulletin of the American Meteorological Society*, 80, 2229-2259.
 42. Kubilay, N., Oguz, T., Koc, M., & Torres, O. (2005). Ground-based assessment of Total Ozone Mapping Spectrometer (TOMS) data for dust transport over the northeastern Mediterranean. *Global Biogeochemical Cycles*, 19, GB1022, doi: 10.1029/2004GB002370, 1-9.
 43. Mallet, M., Pont, V., Lioussé, C., Roger, J.C., & Dubuisson, P. (2006). Simulation of aerosol radiative properties with the ORISAM-RAD model during a pollution event (ESCOMPTE 2001). *Atmospheric Environment*, 40, 7696–7705.
 44. Marticorena, B., Chatenet, B., Rajot, J. L., Traore, S., Coulibaly, M., Diallo, A., Kone, I., Maman, A., NDiaye, T., & Zakou, A. (2010). Temporal variability of mineral dust concentrations over West Africa: analyses of a pluriannual monitoring from the AMMA Sahelian Dust Transect. *Atmospheric Chemistry and Physics*, 10, 8899–8915.
 45. Masmoudi, M., Chaabane, M., Tanré, D., Gouloup, P., Blarel, L., Elleuch, F. (2003). Spatial and temporal variability of aerosol: size distribution and optical properties. *Atmospheric Research*, 66, 1-19.
 46. Moulin, C., & Chiapello, I. (2004). Evidence of the control of summer atmospheric transport of African dust over the Atlantic by Sahel sources from TOMS satellites (1979–2000). *Geophysical Research Letters*, 31, L02107, doi: 10.1029/2003GL018931.
 47. Mueller, D., Wagner, F., Althausen, D., Wandlinger, U., & Ansmann, A. (2000). Physical properties of the Indian plume derived from six-wavelength lidar observations on 25 March 1999 of the Indian Ocean Experiment. *Geophysical Research Letters*, 27, 1403–1406.
 48. Myhre, G., Stordal, F., Johnsrud, M., Diner, D. J., Geogdzhayev, I. V., Haywood, J. M., Holben, B. N., Holzer-Popp, T., Ignatov, A., Kahn, R. A., Kaufman, Y. J., Loeb, N., Martonchik, J. V., Mishchenko, M. I., Nalli, N. R., Remer, L. A., Schroedter-Homscheidt, M., Tanré, D., Torres, O. & Wang, M. (2004). Intercomparison of satellite retrieved aerosol optical depth over ocean during the period September 1997 to December 2000. *Atmospheric Chemistry and Physics*, 5, 1697–1719.

49. Ogunjobi, K.O., He, Z., & Simmer, C. (2008). Spectral aerosol optical properties from AERONET Sun-photometric measurements over West Africa. *Atmospheric Research*, 88, 89–107.
50. Prasad, A.K., Singh, S., Chauhan, S.S., Srivastava, M.K., Singh, R.P., & Singh, R. (2007). Aerosol radiative forcing over the indo-Gangetic plains during major dust storms. *Atmospheric Environment*, 41, 6289-6301.
51. Reid, J.S., Jonsson, H.H., Maring, H.B., Smirnov A., et al. (2003). Comparison of size and morphological measurements of coarse mode dust particles from Africa. *Journal of Geophysical Research* 108 (D19), 8593. doi: 10.1029/2002JD002485.
52. Remer, L. A., Kaufman, Y. J. , Tanre, D. , Mattoo, S. , Chu, D. A. , Martins, J. V. , Li, R.R. , Ichoku, C., Levy, R. C. , Kleidman, R. G. , Eck, T. F. , Vermote, E. ,& Holben, B. N. (2005). The MODIS aerosol algorithm, products and validation. *Journal of Atmospheric Science*, 62(4), 947-973.
53. Satheesh, S.K., Krishna Moorthy, K., Kaufman, Y.J., & Takemura, T. (2006). Aerosol optical depth, physical properties and radiative forcing over the Arabian Sea. *Meteorology and Atmospheric Physics* 91, 45–62.
54. Smirnov, A., Holben, B.N., Savoie, D., Prospero, J.M., Kaufmann, Y.J., Tanre ´, D., Eck, T.F., Slutsker, I.S. (2000). Relationship between column aerosol optical thickness and in situ ground based dust concentrations over Barbados. *Geophysical Research Letters*, 27, 1643–1646.
55. Torres, O., Bhartia, P. K., Herman, J. R., Ahmad, Z., & Gleason J. (1998). Derivation of aerosol properties from satellite measurements of backscattered ultraviolet radiation: Theoretical bases. *Journal of geophysical Research*, 103, 17009–17110.
56. Torres, O., Bhartia, P. K., Herman, J.R., Sinyuk, A., Ginoux, P., Holben, B. (2002). A long term of Aerosol Optical Depth from TOMS observations and comparison with AERONET Measurements. *Journal of the Atmospheric Science*, 58, 398-413.
57. Won, J.G., Yoon, S.C., Kim, S.W., Jefferson, A., Dutton, E.G., & Holben, B.N. (2004). Estimations of direct radiative forcing of Asian dust aerosols with sun/sky radiometer and lidar measurements at Gosan, Korea. *Journal of the Meteorological Society of Japan*, 82, 115–130.
58. Yoon, S.C., Won, J.G., Omar, A.H., Kim, S.W., & Sohn, B.J. (2005). Estimation of the radiative forcing by key aerosol types in worldwide locations using column model and AERONET data. *Atmospheric Environment*, 39, 6620-6630.
59. Yoshioka, M., Mahowald, J., Dufresne, L., & Luo, C. (2005). Simulation of absorbing aerosol indices for African dust. *Journal of Geophysical Research*, 110, D18S17, doi: 10.1029/2004JD005276.
60. Yu, X., Zhu, B., & Zhang, M. (2009). Seasonal variability of aerosol optical properties over Beijing *Atmospheric Environment*, 43, 4095–4101.
61. Zhao, T.X.P., Stowe, L.L., Smirnov, A., Crosby, D., Sapper, J., & McClain, C.R. (2002). Development of a global validation package for satellite oceanic aerosol optical thickness retrieval based on AERONET observations and its application to NOAA/NESDIS operational aerosol retrievals. *Journal of Atmospheric Sciences*, 59 (3), 294–312.

Table 1a : Monthly averages of Rainfall (mm), Temperature (°C) and Relative humidity (%) measure at the four stations during 2005-2008.

(a) Rainfall (mm)													
	Jan	Feb	Mar	Apr	May	Jun	Jul	Aug	Sep	Oct	Nov	Dec	mmyr ⁻¹
Agoufou	0.1	0.1	0.6	2.9	8.7	37.8	103.2	109.5	57.0	12.9	0.6	0.3	333.0
Banizoumbou	0.1	0.6	3.9	5.7	34.7	68.8	154.3	170.8	92.2	9.7	0.7	0.5	540.8
Cape Verde	5.3	3.8	1.3	0.7	0.6	0.8	0.8	14.1	33.6	6.5	2.5	1.6	69.5
Ilorin	6.2	18.2	57.4	107.1	151.6	189.0	149.1	152.9	211.1	130.2	4.6	7.6	1185.0
(b)Temperature													
	Jan	Feb	Mar	Apr	May	Jun	Jul	Aug	Sep	Oct	Nov	Dec	Average
Agoufou	24.8	27.4	30.6	33.4	35.5	34.2	31.2	29.6	30.8	31.9	28.6	25.1	30.26
Banizoumbou	24.3	27.3	30.9	33.8	34.0	31.5	29.0	27.9	29.0	30.8	27.9	25.0	29.28
Cape Verde	21.4	21.1	21.6	21.9	22.5	23.4	24.6	26.0	26.6	26.1	24.5	22.7	23.53
Ilorin	26.0	28.1	28.3	28.1	27.0	25.5	24.5	24.5	24.6	25.6	26.2	25.7	26.18
c. Relative Humidity (%)													
	Jan	Feb	Mar	Apr	May	Jun	Jul	Aug	Sep	Oct	Nov	Dec	Average
Agoufou	22	19	19	21	23	42	56	63	56	36	22	26	34
Banizoumbou	24	20	21	29	44	56	67	72	68	48	31	27	42
Cape Verde	70	71	71	71	73	75	75	75	77	75	73	71	73
Ilorin	61	71	64	74	75	84	85	86	85	82	76	55	75

Table 2 : Statistics of daily AERONET AOD (440nm) for the period 2005-2009, including the mean (M), the standard deviation (σ), the median (ψ), the minimum (min), the maximum (max), the variance (υ), the 5th and 95th percentile lower and upper confidence level (P5 and P95).

	N _{days}	M	σ	min	ψ	max	υ	P5LCL/UCL	P95LCL/UCL
Agoufou	1092	0.52	0.39	0.05	0.43	3.89 26 th May 2006	0.15	0.150/0.150	0.139/0.163
Banizoumbou	1358	0.57	0.43	0.05	0.45	3.61 7 th Jan 2005	0.18	0.180/0.181	0.168/0.194
Cape Verde	1032	0.37	0.24	0.03	0.32	1.67 8 th Jan 2005	0.05	0.057/0.057	0.052/0.062
Ilorin	1159	0.75	0.49	0.07	0.62	3.87 11 th Mar 2006	0.24	0.243/0.244	0.223/0.265

Table 3 : Statistics of daily TOMS A1.

	N _{days}	M	σ	min	ψ	Max	υ	P5LCL/UCL	P95LCL/UCL
Agoufou	859	0.58	0.33	0.20	0.52	3.25 4 th April 2007	0.11	0.109/0.110	0.101/0.121
Banizoumbou	1074	0.85	0.41	0.25	0.75	3.40 4 th April 2007	0.17	0.164/0.165	0.151/0.179
Cape Verde	1077	0.84	0.45	0.25	0.75	3.25 14 th May 2005	0.21	0.205/0.206	0.189/0.224
Ilorin	864	1.07	0.54	0.33	1.00	3.13 3 rd Mar 2007	0.29	0.287/0.288	0.262/0.317

Table 4 : Statistics of daily MODIS-terra AOD (440nm).

	N _{days}	M	σ	min	ψ	Max	υ	P5LCL/UCL	P95LCL/UCL
Agoufou	592	0.56	0.47	0.02	0.43	4.70 4 th April 2007	0.22	0.221/ 0.223	0.198/ 0.249
Banizoumbou	441	0.69	0.57	0.04	0.51	3.93 2 nd Jan 2005	0.32	0.321/ 0.323	0.283/ 0.369
Cape Verde	284	0.37	0.29	0.03	0.31	3.31 8 th Jan 2005	0.09	0.086/0.087	0.073/0.102
Ilorin	327	0.88	0.60	0.15	0.73	4.16 11 th Mar 2006	0.36	0.357/0.361	0.309/0.420

Table 5 : Statistics of daily MODIS-aqua AOD (440nm).

	N _{days}	M	σ	min	ψ	Max	υ	P5LCL/UCL	P95LCL/UCL
Agoufou	397	0.57	0.41	0.08	0.46	3.11 11 th May 2007	0.17	0.169/0.171	0.148/0.196
Banizoumbou	437	0.62	0.50	0.06	0.47	3.94 7 th Jan 2005	0.25	0.251/0.253	0.221/0.289
Cape Verde	279	0.39	0.30	0.03	0.34	3.10 8 th Jan 2005	0.09	0.091/0.092	0.078/0.108
Ilorin	305	0.81	0.51	0.13	0.67	3.15 10 th Mar 2006	0.26	0.259/0.262	0.223/0.306

Table 6 : Summary of the AERONET AOD with TOMS AI, MODIS-Terra and Aqua linear relationships from daily observations in the form $AOD_{satellite} = A * AOD_{AERONET} + B$. Also computed are the corresponding number of days, correlation coefficients, and the standard errors in the slopes and intercepts.

	N _{days}	Regression equation	R	R ²	Std Error (intercept)	Std Error (slope)
Agoufou	859	AI: $y = 0.804 x + 0.420$	0.72	0.52	0.040	0.001
		Terra: $y = 1.059 x + 0.057$	0.96	0.93	0.009	0.012
		Aqua: $y = 1.020 x + 0.195$	0.96	0.92	0.010	0.015
Banizoumbou	1012	AI: $y = 0.601 x + 0.502$	0.67	0.45	0.010	0.009
		Terra: $y = 1.051 x + 0.010$	0.93	0.87	0.013	0.015
		Aqua: $y = 1.067 x + 0.013$	0.94	0.89	0.011	0.014
Cape Verde	761	AI: $y = 0.838 x + 0.224$	0.63	0.40	0.003	0.011
		Terra: $y = 1.010 x + 0.002$	0.98	0.96	0.006	0.014
		Aqua: $y = 1.032 x + 0.007$	0.96	0.92	0.005	0.012
Ilorin	836	AI: $y = 0.812 x + 0.451$	0.76	0.58	0.015	0.021
		Terra: $y = 1.022 x + 0.009$	0.93	0.88	0.031	0.031
		Aqua: $y = 0.979 x + 0.013$	0.98	0.96	0.017	0.017

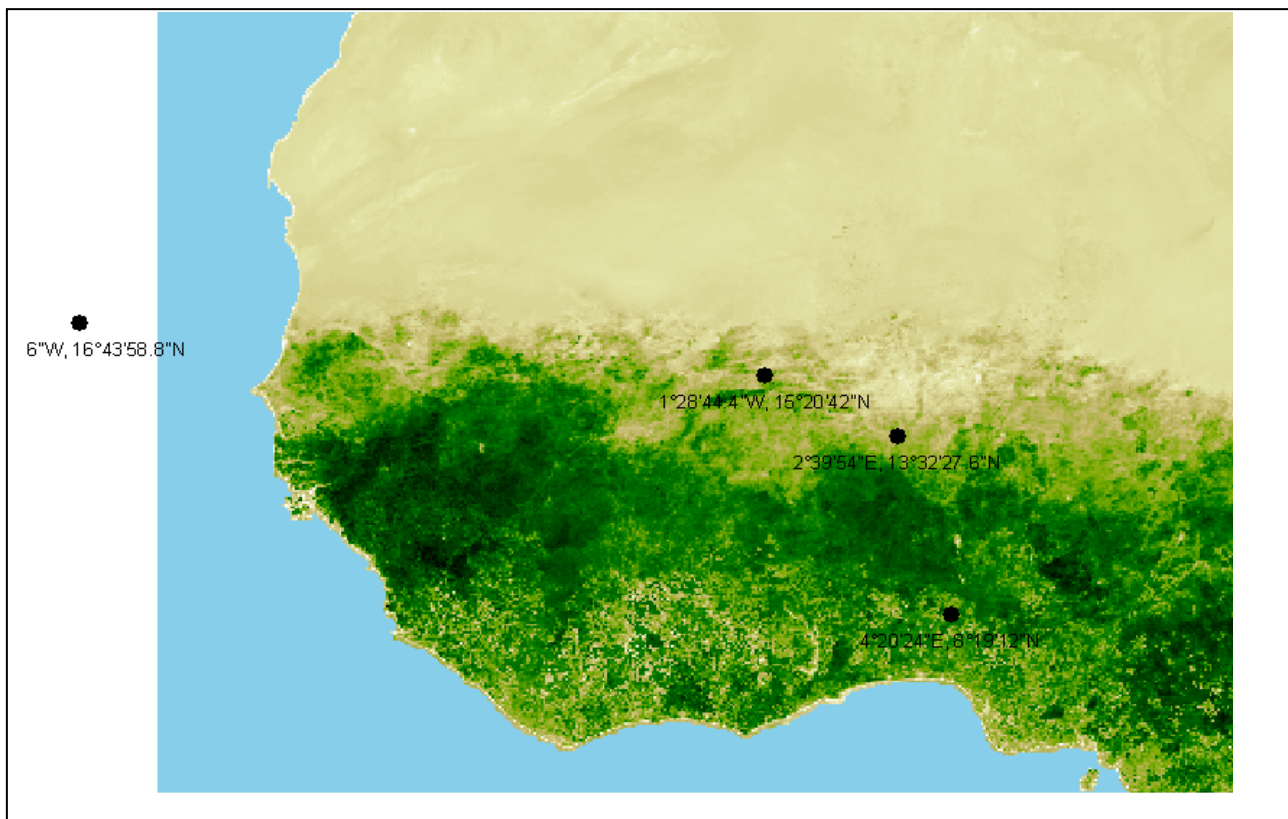


Figure 1 : Maps of locations.

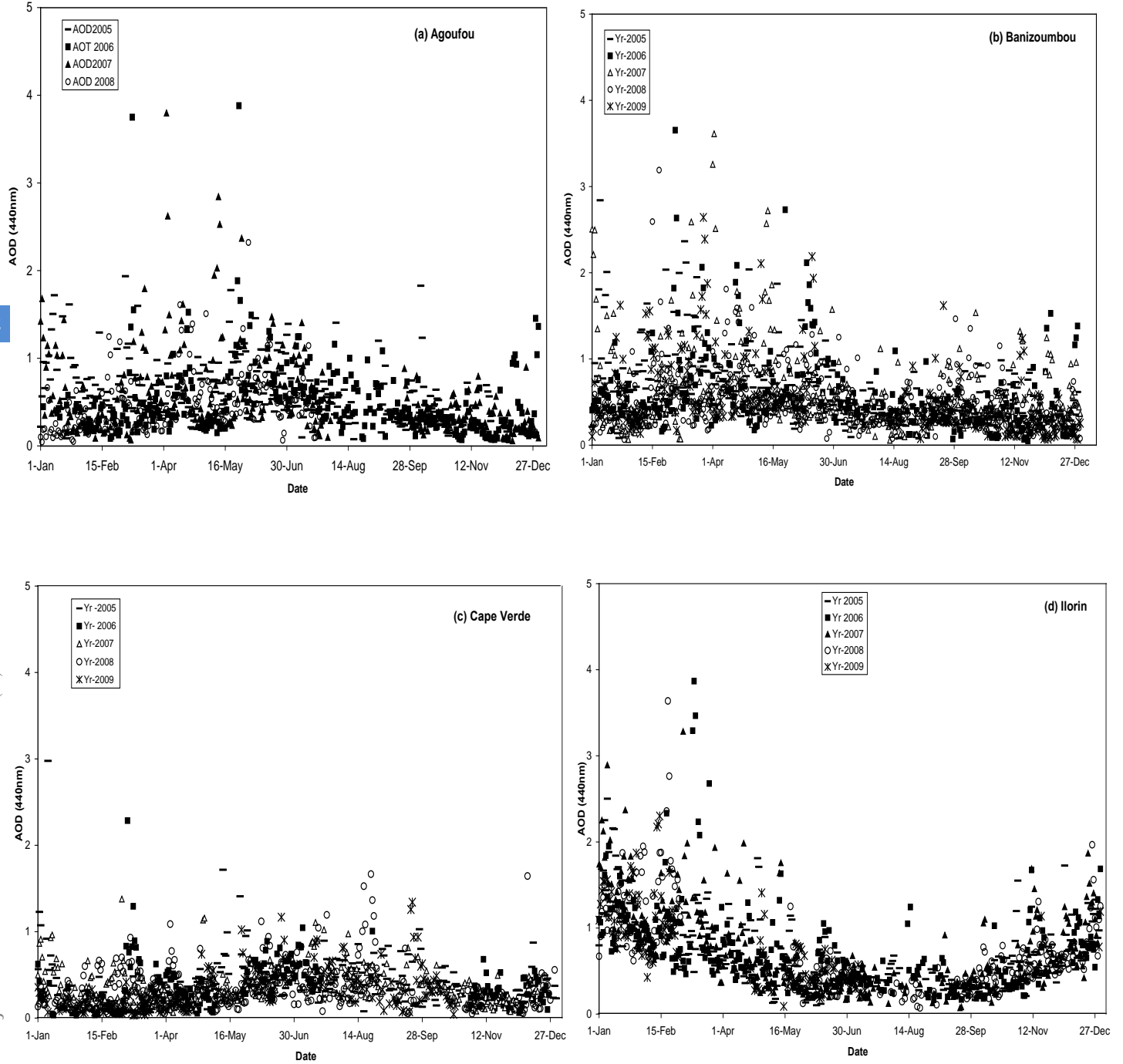


Figure 2 : Day-day variability of AERONET aerosol optical depth (440nm) in the stations under consideration: (a) Agoufou, (b) Banizoumbou, (c) Cape Verde and (d) Ilorin.

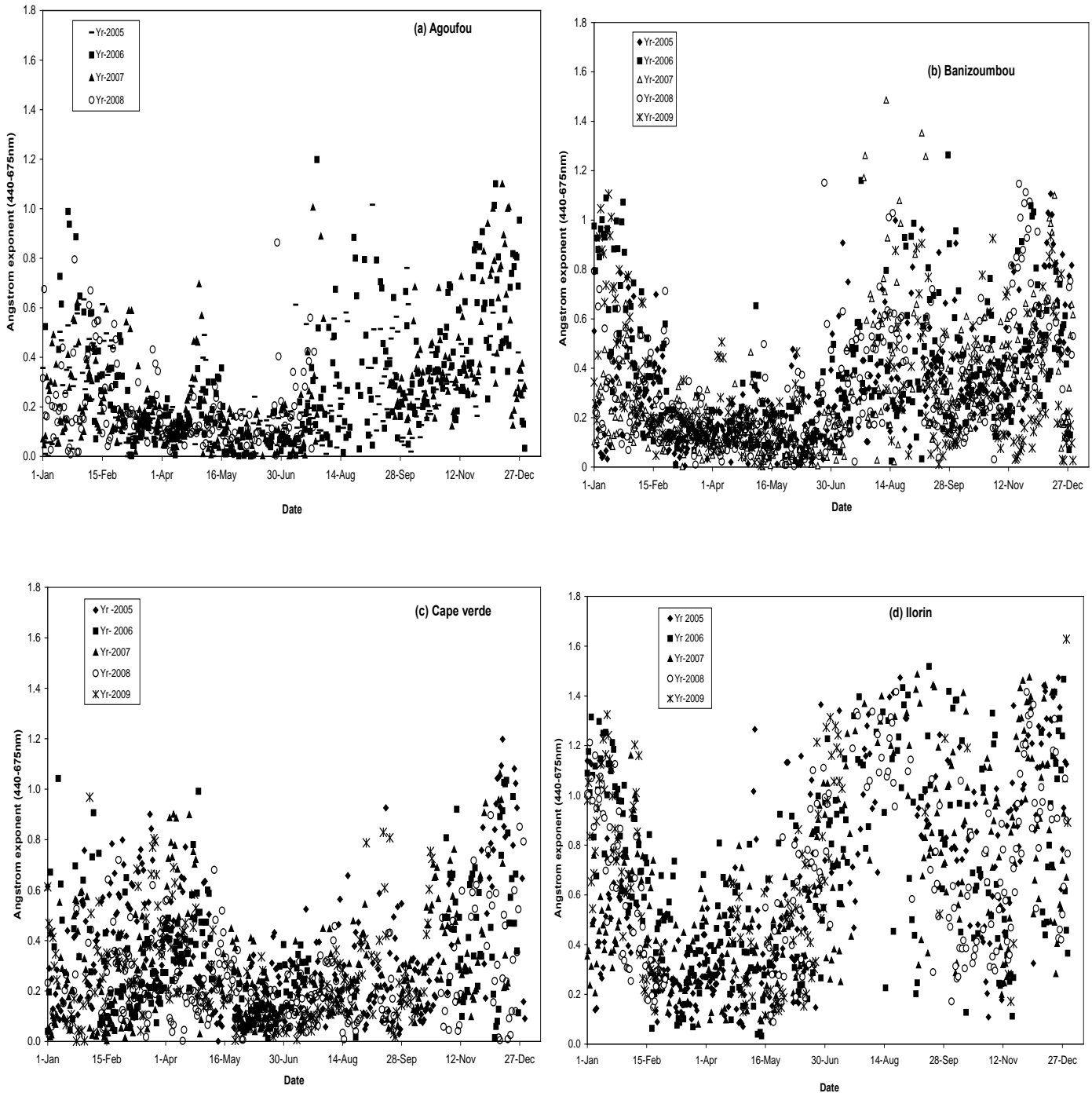


Figure 3 : Day-to-day variation of $\alpha_{440-675nm}$ at Agoufou, Banizoumbou, Cape Verde and Ilorin.

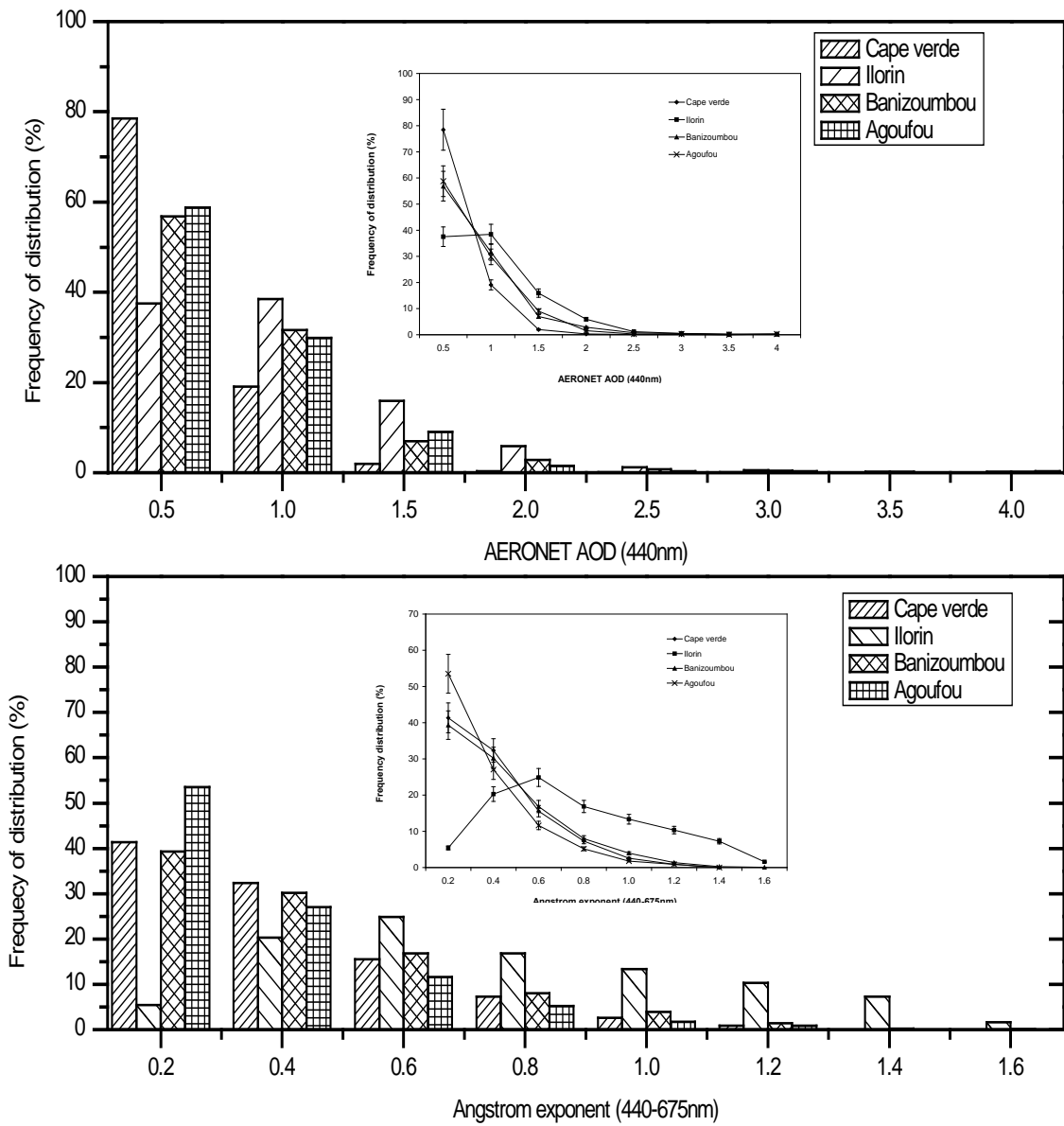


Figure 4 : Frequency distribution of AERONET aerosol optical depth in percentage and Angstrom exponent during 2005-2009.

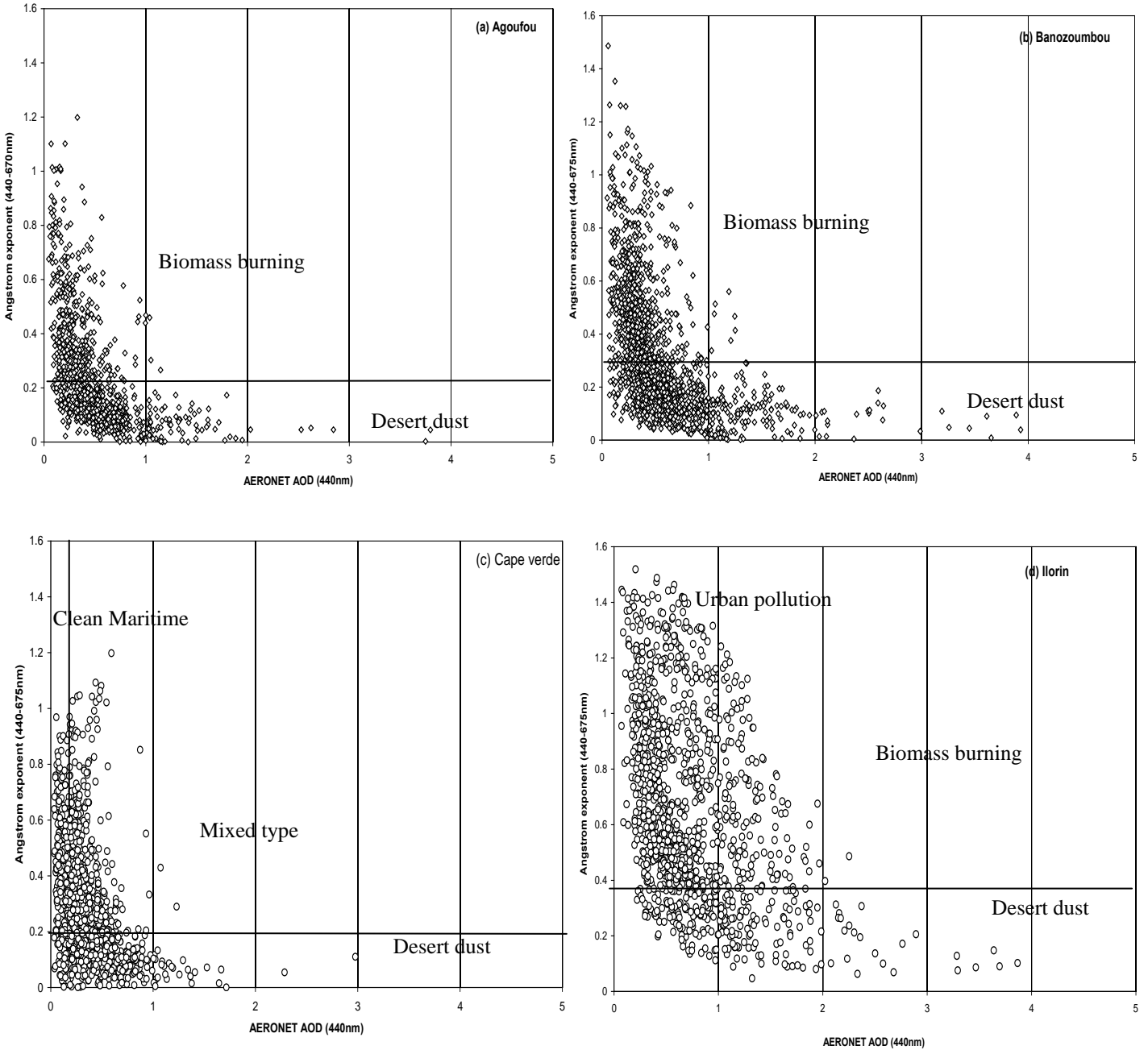


Figure 5: Scatter-gram of daily averages of AERONET aerosol optical depth against Angstrom exponent (440-675nm).

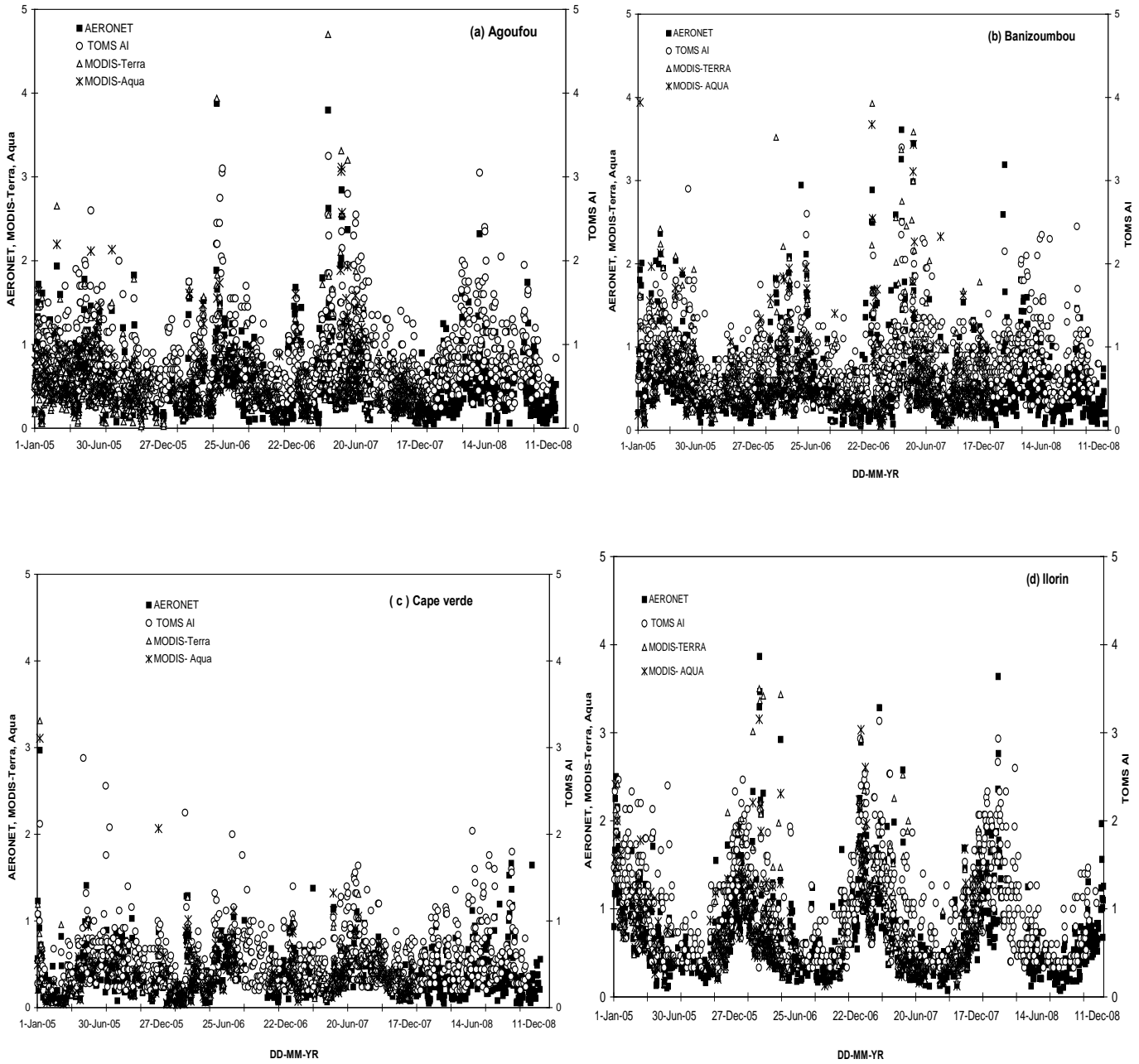


Figure 6 : Day-to-day comparison of AERONET, MODIS-Terra, MODIS-Aqua aerosols optical depth and TOMS AI observations at (a) Agoufou, (b) Banizoumbou, (c) Cape Verde, and (d) Ilorin.

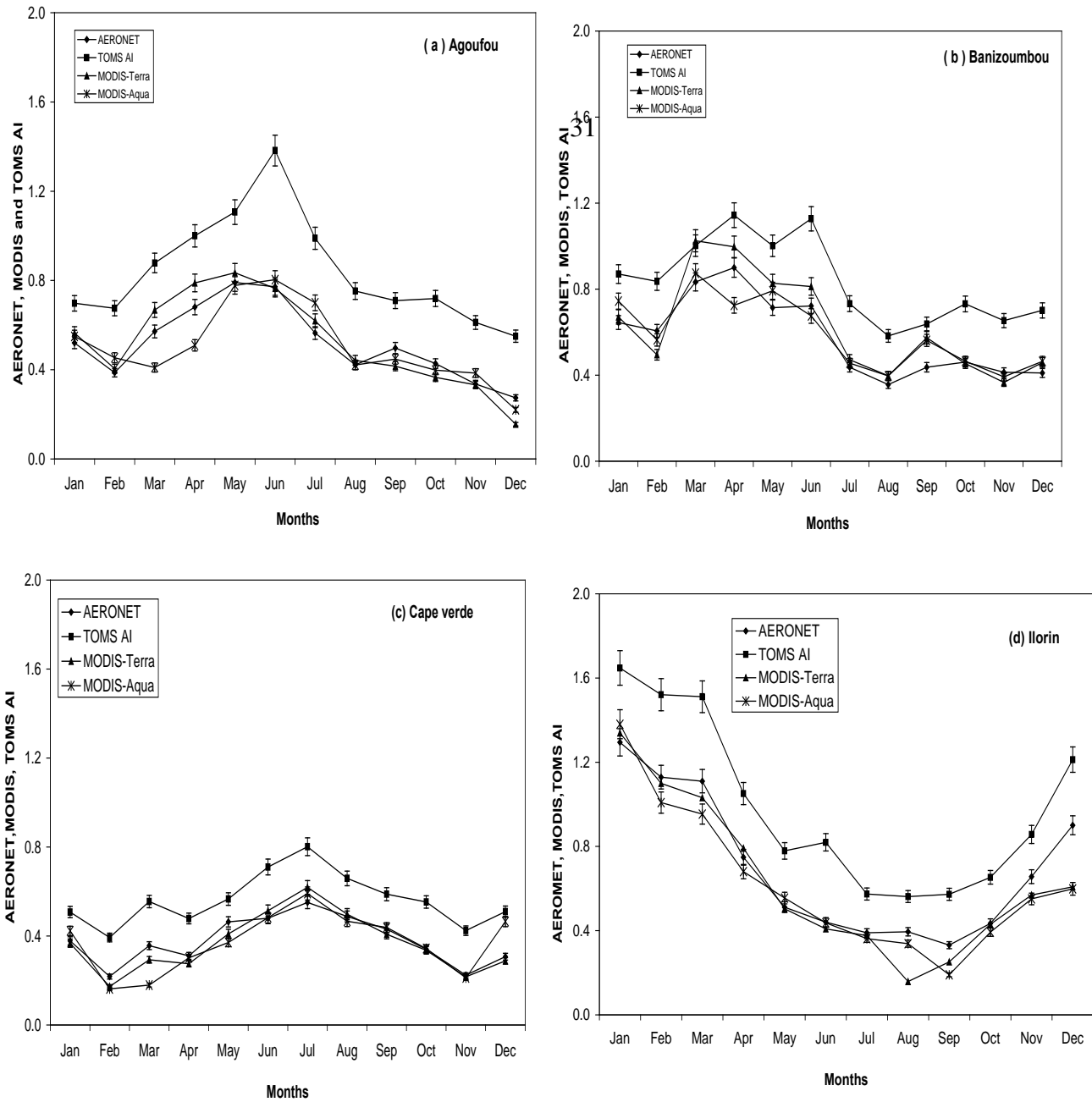


Figure 7: Long-term monthly averages of aerosol optical depth from satellite and ground-based AERONET observations for at (a) Agoufou, (b) Banizoumbou, (c) Cape Verde, and (d) Ilorin. Also shown are the error bars corresponding to 5% standard deviation.

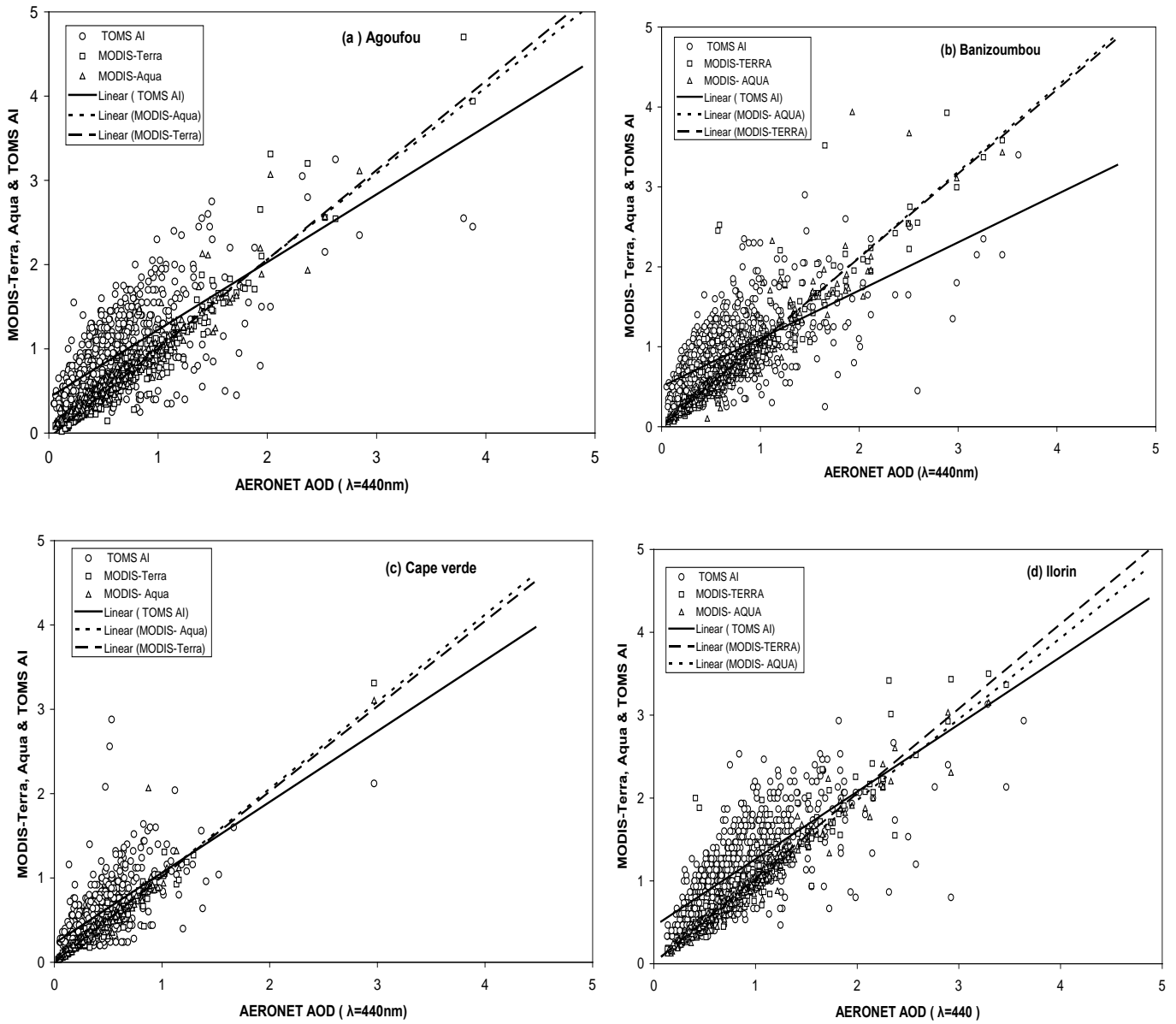


Figure 8 : Regression plots of satellite observations from MODIS & TOMS against ground-based AERONET observations for (a) Agoufou, (b) Banizoumbou, (c) Cape Verde, (d) Ilorin.